

## *Ab initio* Hartree-Fock calculations of crystalline systems using full-symmetry analysis of basis-set expansions

Thomas H. Upton and William A. Goddard III

*Arthur Amos Noyes Laboratory of Chemical Physics, California Institute of Technology, Pasadena, California 91125*

(Received 26 November 1979)

A technique is presented for carrying out *ab initio* Hartree-Fock calculations on systems of infinite three-dimensional periodicity. The method represents an adaptation of standard molecular basis-set expansion techniques and fully utilizes translational and point-group symmetry to simplify the calculations. It is shown that the expression for total energy may be written as a sum of pairwise interactions between neutral charge units consisting of a nucleus and a localized compensating electronic charge. The resulting sums are rapidly convergent. The technique is illustrated with sample calculations on face-centered-cubic lattices of hydrogen, lithium, and sodium. Generalization to systems of lower symmetry is discussed.

### I. INTRODUCTION

In recent years it has become increasingly apparent that existing theoretical techniques are inadequate for the detailed study of electronic states at solid surfaces and defect sites. Semiempirical band-calculation methods allow treatment of long-range periodicity,<sup>1</sup> but do not permit the evaluation of total energies and hence cannot differentiate unambiguously between possible surface or defect structures. *Ab initio* methods do not suffer from this limitation and have been successful in the study of localized chemisorptive bonding states on metal<sup>2</sup> and semiconductor<sup>3</sup> surfaces. However, these calculations have required that the surface be modeled using a finite cluster of atoms. This restriction leaves these methods incapable of considering a host of phenomena whose characteristics are intimately related to the two-dimensional symmetry of the surface.

We feel that the solution to this dilemma lies in the development of an *ab initio* variational technique that includes full two-dimensional periodicity. Ultimately it will be necessary to allow systematic examination of electron correlation (many-body) effects; however, as a first step in this program we have considered a simpler problem: Exact Hartree-Fock (HF) calculations on three-dimensional periodic systems. In this paper we generalize the *ab initio* techniques used previously in cluster studies<sup>4</sup> to take full account of periodicity. The resulting energy expressions retain the numerical simplicity of basis-set expansion techniques<sup>5</sup> and may be cast in a rapidly convergent form. To illustrate its application, we report the results of calculations on some simple systems: Face-centered-cubic arrays of hydrogen, lithium, and sodium. While the development presented here is specific to systems of three-dimensional periodicity, extension to systems of

lesser periodicity is straightforward, and we conclude with a brief discussion of methods by which this may be done.

### II. HARTREE-FOCK FORMALISM

#### A. Wave functions and Hamiltonian

The construction of general one-electron wave functions is begun by defining a *basis* of Bloch orbitals for each wave vector  $\vec{k}$  as

$$\varphi_{\vec{k}}^a(\vec{r}) = \sum_{\mu}^N e^{i\vec{k}\cdot\vec{R}_{\mu}} \phi^a(\vec{r} - \vec{R}_{\mu}), \quad (1)$$

where (for simplicity) we have assumed a single atom per unit cell, and the sum runs over all  $N$  atoms (cells) of the semi-infinite lattice. Here the  $\phi^a(\vec{r})$  are basis functions centered on the atoms and located by the vector  $\vec{R}_{\mu}$ . We will take them to be linear combinations of Cartesian Gaussians,

$$\phi^a(\vec{r}) = x^l y^p z^q e^{-\alpha r^2} / \sqrt{N_a}, \quad (2)$$

where  $l$ ,  $p$ , and  $q$  are integers,  $\alpha$  is a variable scale factor, and  $N_a$  is the normalization constant. The  $\varphi_{\vec{k}}^a$  are normalized but not orthogonal (for a given value of  $\vec{k}$ ). The one-electron functions (Hartree-Fock orbitals) are obtained from the basis functions as

$$\psi_{\vec{k}n}(\vec{r}) = \eta_{\vec{k}n}^{-1/2} \sum_a^m C_{\vec{k}n}^a \varphi_{\vec{k}}^a(\vec{r}), \quad (3)$$

where the normalization factor is

$$\begin{aligned} \eta_{\vec{k}n} &= \sum_{a,b}^m \sum_{\mu,\nu}^N C_{\vec{k}n}^{*a} C_{\vec{k}n}^b e^{i\vec{k}\cdot(\vec{R}_{\mu}-\vec{R}_{\nu})} \\ &\quad \times \langle \phi^a(\vec{r} - \vec{R}_{\nu}) | \phi^b(\vec{r} - \vec{R}_{\mu}) \rangle \\ &= N \sum_{a,b}^m \sum_{\sigma}^N C_{\vec{k}n}^{*a} C_{\vec{k}n}^b e^{i\vec{k}\cdot\vec{R}_{\sigma}} \langle \phi^a(\vec{r}) | \phi^b(\vec{r} - \vec{R}_{\sigma}) \rangle. \end{aligned} \quad (4)$$

In (3) the sum is over the  $m$  (nonorthogonal) basis functions for each  $\vec{k}$ , and the subscript  $n$  identifies

the band (i.e., root of the Hamiltonian matrix for a given  $\vec{k}$ ). The coefficients  $C_{\vec{k}n}^a$  are obtained variationally (solutions of the matrix HF equations). These one-electron wave functions (3) may be combined to form the single Slater determinant wave functions relevant to this study.

$$\Psi_{\text{CS}} = \alpha [\psi_{\vec{k}n_1}(\vec{r}_1) \psi_{\vec{k}n_2}(\vec{r}_2) \cdots \psi_{\vec{k}n_f}(\vec{r}_{Np-1}) \psi_{\vec{k}n_f}(\vec{r}_{Np}) \chi_{\text{CS}}], \quad (5)$$

$$\Psi_{\text{HS}} = \alpha [\psi_{\vec{k}n_1}(\vec{r}_1) \psi_{\vec{k}n_2}(\vec{r}_2) \cdots \psi_{\vec{k}n_{f-1}}(\vec{r}_{Np-1}) \times \psi_{\vec{k}n_f}(\vec{r}_{Np}) \chi_{\text{HS}}]. \quad (6)$$

Here  $\Psi_{\text{CS}}$  and  $\Psi_{\text{HS}}$  are wave functions for closed-shell ( $S=0$ ) and high-spin ( $S=Np/2$ ) states for an array of  $N$  atoms, each with  $p$  valence electrons, and the  $\chi_{\text{CS}}$  and  $\chi_{\text{HS}}$  are the appropriate spin functions.<sup>6</sup>

The total electronic Hamiltonian is

$$\mathcal{H} = \sum_i^{Np} h_i + \sum_{j>k}^{Np} \frac{1}{|\vec{r}_j - \vec{r}_k|},$$

where  $h_i$  is the one-electron operator

$$h_i = -\frac{1}{2} \nabla_i^2 - \sum_{\mu}^N \left( \frac{Z_{\mu}}{|\vec{R}_{\mu} - \vec{r}_i|} - V_{\mu}^{\text{core}} \right), \quad (7)$$

and  $V_{\mu}^{\text{core}}$  is the potential for the core electrons on center  $\mu$ . The total energies of  $\Psi_{\text{CS}}$  and  $\Psi_{\text{HS}}$  are

$$E = \sum_{\vec{k}n}^{Np/f} f h_{\vec{k}n, \vec{k}n} + \sum_{\vec{k}n, \vec{k}'n'}^{Np/f} (A J_{\vec{k}n, \vec{k}'n'} - B K_{\vec{k}n, \vec{k}'n'}) + \sum_{\mu>\nu}^N \frac{Z_{\mu} Z_{\nu}}{|\vec{R}_{\mu} - \vec{R}_{\nu}|}, \quad (8)$$

and the orbital eigenvalues are

$$\epsilon_{\vec{k}n} = h_{\vec{k}n, \vec{k}n} + \frac{2}{f} \sum_{\vec{k}'n'}^{Np/f} (A J_{\vec{k}n, \vec{k}'n'} - B K_{\vec{k}n, \vec{k}'n'}). \quad (9)$$

Expressions (8) and (9) permit a very general class of wave functions<sup>7</sup> of which two special cases are considered here:

$$f=2, \quad A=2, \quad B=1 \quad \text{for } \Psi_{\text{CS}},$$

$$f=1, \quad A=\frac{1}{2}, \quad B=\frac{1}{2} \quad \text{for } \Psi_{\text{HS}}.$$

The  $\vec{k}n$  are over all *occupied* orbitals. The first term in (8) is a sum of one-electron energies,

$$\begin{aligned} \sum_{\vec{k}n}^{Np/f} f h_{\vec{k}n, \vec{k}n} &= \sum_{\vec{k}n}^{Np/f} f \eta_{\vec{k}n}^{-1} \sum_{a,b}^m C_{\vec{k}n}^{*a} C_{\vec{k}n}^b \langle \phi_{\vec{k}}^a(\vec{r}) | h | \phi_{\vec{k}}^b(\vec{r}) \rangle \\ &= fN \sum_{\vec{k}n}^{Np/f} \eta_{\vec{k}n}^{-1} \sum_{a,b}^m \sum_{\sigma}^N C_{\vec{k}n}^{*a} C_{\vec{k}n}^b e^{i\vec{k} \cdot \vec{R}_{\sigma}} \\ &\quad \times \langle \phi^a(\vec{r}) | h | \phi^b(\vec{r} - \vec{R}_{\sigma}) \rangle \\ &= fN \sum_{a,b}^m \sum_{\sigma}^N D_{1\sigma}^{ab} h_{1\sigma}^{ab}, \end{aligned} \quad (10)$$

where

$$D_{\mu\nu}^{ab} = \sum_{\vec{k}n}^{Np/f} \eta_{\vec{k}n}^{-1} C_{\vec{k}n}^{*a} C_{\vec{k}n}^b e^{i\vec{k} \cdot (\vec{R}_{\nu} - \vec{R}_{\mu})}, \quad (11)$$

$$h_{\mu\nu}^{ab} = \langle \phi^a(\vec{r} - \vec{R}_{\mu}) | h | \phi^b(\vec{r} - \vec{R}_{\nu}) \rangle,$$

and  $\sigma=1$  refers to the atom chosen as the origin. The quantities  $D_{\mu\nu}^{ab}$  may be identified as elements of the one-particle density matrix upon noting that

$$\begin{aligned} \rho(\vec{r}) &= f \sum_{\vec{k}n}^{Np/f} \psi_{\vec{k}n}^*(\vec{r}) \psi_{\vec{k}n}(\vec{r}) \\ &= f \sum_{a,b}^m \sum_{\mu,\nu}^N \sum_{\vec{k}n}^{Np/f} \eta_{\vec{k}n}^{-1} C_{\vec{k}n}^{*a} C_{\vec{k}n}^b e^{i\vec{k} \cdot (\vec{R}_{\nu} - \vec{R}_{\mu})} \\ &\quad \times \phi^a(\vec{r} - \vec{R}_{\mu}) \phi^b(\vec{r} - \vec{R}_{\nu}) \\ &= f \sum_{a,b}^m \sum_{\mu,\nu}^N D_{\mu\nu}^{ab} \phi^a(\vec{r} - \vec{R}_{\mu}) \phi^b(\vec{r} - \vec{R}_{\nu}). \end{aligned}$$

In addition, we have

$$\rho(\vec{r}) = \sum_{\nu}^N \rho_{\nu}(\vec{r}),$$

where

$$\rho_{\nu}(\vec{r}) = f \sum_{a,b}^m \sum_{\mu}^N D_{\mu\nu}^{ab} \phi^a(\vec{r} - \vec{R}_{\mu}) \phi^b(\vec{r} - \vec{R}_{\nu}).$$

Integrating over all space leads to

$$p = \int d^3\vec{r} \rho_{\nu}(\vec{r}) = f \sum_{a,b}^m \sum_{\mu}^N D_{\mu\nu}^{ab} S_{\mu\nu}^{ab}.$$

Thus,  $\rho_{\nu}(\vec{r})$  is the density function for the  $p$  electrons near atom  $\nu$ .

Applying (11) to the two-electron Coulomb  $J_{\vec{k}n, \vec{k}'n'}$  and exchange  $K_{\vec{k}n, \vec{k}'n'}$  sums in (8) leads to

$$\sum_{\vec{k}n, \vec{k}'n'}^{Np/f} (A J_{\vec{k}n, \vec{k}'n'} - B K_{\vec{k}n, \vec{k}'n'}) = N \sum_{a,b}^m \sum_{\sigma}^N D_{1\sigma}^{ab} \sum_{c,d}^m \sum_{\mu,\nu}^N D_{\mu\nu}^{cd} [A (a^{\dagger} b^{\sigma} | c^{\mu} d^{\nu}) - B (a^{\dagger} c^{\mu} | b^{\sigma} d^{\nu})] \quad (12)$$

using the notation

$$(a^{\sigma} b^{\nu} | c^{\mu} d^{\nu}) \equiv \int \phi^a(\vec{r}_1 - \vec{R}_{\sigma}) \phi^b(\vec{r}_1 - \vec{R}_{\nu}) d^3\vec{r}_1 \int \frac{1}{|\vec{r}_1 - \vec{r}_2|} \phi^c(\vec{r}_2 - \vec{R}_{\mu}) \phi^d(\vec{r}_2 - \vec{R}_{\nu}) d^3\vec{r}_2.$$

Combining the above equations leads to

$$E = N \sum_{a,b}^m \sum_{\sigma}^N D_{1\sigma}^{ab} \left( f h_{1\sigma}^{ab} + \sum_{c,d}^m \sum_{\mu,\nu}^N D_{\mu\nu}^{cd} [A(a^1 b^\sigma | c^\mu d^\nu) - B(a^1 c^\mu | b^\sigma d^\nu)] \right) + \sum_{\mu>\nu}^N \frac{Z_\mu Z_\nu}{|\vec{R}_\mu - \vec{R}_\nu|} \quad (13)$$

and

$$\epsilon_{\vec{k}\vec{n}} = N \eta_{\vec{k}\vec{n}}^{-1} \sum_{\sigma}^m \sum_{a,b}^N C_{\vec{k}\vec{n}}^{*a} C_{\vec{k}\vec{n}}^b e^{i\vec{k}\cdot\vec{R}_\sigma} \left( h_{1\sigma}^{ab} + \frac{2}{f} \sum_{c,d}^m \sum_{\mu,\nu}^N D_{\mu\nu}^{cd} [A(a^1 b^\sigma | c^\mu d^\nu) - B(a^1 c^\mu | b^\sigma d^\nu)] \right). \quad (14)$$

For systems with inversion symmetry,

$$\phi_{\vec{k}\vec{n}} = \phi_{-\vec{k}\vec{n}}^*$$

and

$$\epsilon_{\vec{k}\vec{n}} = \epsilon_{-\vec{k}\vec{n}}.$$

As a result, we may avoid dealing with complex quantities by redefining (14) as

$$\frac{1}{2}(\epsilon_{\vec{k}\vec{n}} + \epsilon_{-\vec{k}\vec{n}}) = N(\eta_{\vec{k}\vec{n}} + \eta_{-\vec{k}\vec{n}})^{-1} \sum_{\sigma}^m \sum_{a,b}^N \text{Re}(C_{\vec{k}\vec{n}}^{*a} C_{\vec{k}\vec{n}}^b e^{i\vec{k}\cdot\vec{R}_\sigma}) \left( h_{1\sigma}^{ab} + \frac{2}{f} \sum_{c,d}^m \sum_{\mu,\nu}^N D_{\mu\nu}^{cd} [A(a^1 b^\sigma | c^\mu d^\nu) - B(a^1 c^\mu | b^\sigma d^\nu)] \right).$$

### B. The density matrix

The form of (11) for the density matrix elements, while general, is not particularly useful, as it defines  $N^2 m^2$  distinct elements. It is immediately apparent that this value is too large since  $D_{\mu\nu}^{ab}$  depends only on  $\vec{R}_\nu - \vec{R}_\mu$ . Thus, there are at most the  $Nm^2$  distinct values  $D_{1\sigma}^{ab}$ .

Consideration of point-group symmetry allows this set to be reduced still further. The atoms surrounding atom 1 may be broken into  $\lambda$  "shells," where each atom in a shell has the same value for  $|\vec{R}_\sigma|$  and is related to the others by an operation of the lattice-point group. Thus, Eq. (11) may be rewritten

$$D_{1\sigma}^{ab} = \sum_s^{\text{unique}} \left( \sum_j^{t_s} \eta_{n\vec{k}_j}^{-1} C_{n\vec{k}_j}^{*a} C_{n\vec{k}_j}^b e^{i\vec{k}_j \cdot \vec{R}_\sigma} \right),$$

where the sum over  $\vec{k}\vec{n}$  has been broken into an outer sum over stars of vectors  $s$ , and an inner sum  $j$  over the  $t_s$  members of each of these stars (and occupied bands). But, from the definition of a star, this is equivalent to

$$D_{1\sigma}^{ab} = \sum_s^{\text{unique}} \frac{1}{g_s} \sum_j^{\mathcal{G}} \eta_{n\vec{k}_j}^{-1} C_{n\vec{k}_j}^{*a} C_{n\vec{k}_j}^b e^{i(\vec{R}_j \cdot \vec{R}_\sigma)}, \quad (15a)$$

where, for simplicity,

$$K_j = \mathcal{O}_j(\vec{k}_s),$$

and the inner sum is over the operations  $\mathcal{O}_j$  of the lattice-point group  $\mathcal{G}$ . Using the reciprocal relationship between  $\vec{k}$  and  $\vec{r}$  this becomes

$$D_{1\sigma}^{ab} = \sum_s^{\text{unique}} \frac{1}{g_s} \sum_j^{\mathcal{G}} \eta_{n\vec{k}_s}^{-1} C_{n\vec{k}_s}^{*a} C_{n\vec{k}_s}^b e^{i\vec{k}_s \cdot \mathcal{O}_j^{-1}(\vec{R}_\sigma)}, \quad (15b)$$

where, for example,

$$A_j = \mathcal{O}_j^{-1}(a).$$

The leading factors  $g_s$  and  $g_\sigma$  in (15a) and (15b) are degeneracy factors from the application of the  $\mathcal{O}_j$  to vectors in  $\vec{k}$  and  $\vec{r}$  space, respectively. From (15b) we have, for a particular atom  $\sigma' = \mathcal{O}_\sigma(\sigma)$ ,

$$\begin{aligned} D_{1\sigma'}^{a'b'} &= D_{1\mathcal{O}_\sigma(\sigma)}^{A_j B_j} = \sum_s^{\mathcal{G}} \frac{1}{g_\sigma} \sum_j^{\mathcal{G}/i} \eta_{n\vec{k}_s}^{-1} C_{n\vec{k}_s}^{*A_j} C_{n\vec{k}_s}^{B_j} \\ &\quad \times \exp[i\vec{k}_s \cdot \mathcal{O}_\sigma^{-1}(\vec{R}_\sigma)] \\ &= D_{1\sigma}^{ab}. \end{aligned}$$

Thus, only a single atom in any particular shell need be considered, reducing the number of necessary elements to  $\lambda m^2$  (where  $\lambda$  is the number of shells). Once again, for systems with inversion symmetry, it is convenient to redefine (15b) as

$$D_{1\sigma}^{ab} = 2 \sum_s^{\mathcal{G}/i} \frac{1}{g_\sigma} \sum_j^{\mathcal{G}/i} \eta_{n\vec{k}_s}^{-1} \text{Re}(C_{n\vec{k}_s}^{*A_j} C_{n\vec{k}_s}^{B_j} e^{i\vec{k}_s \cdot \mathcal{O}_j^{-1}(\vec{R}_\sigma)}),$$

where  $\mathcal{G}/i$  is the pure rotation subgroup of  $\mathcal{G}$ , and the inversion symmetry has been explicitly included in obtaining the real function. For these cases,

$$D_{1\sigma}^{ab} = D_{1\sigma}^{ba},$$

and only  $\frac{1}{2}\lambda m(m+1)$  elements are unique among the density matrix elements.

### C. Matrix elements

An additional difficulty arising from the use of Eqs. (13) and (14) is that they appear to require an exorbitant number of one- and two-electron matrix elements. The problem of defining a unique set of one-electron matrix elements has been dealt with in detail by Slater and Koster,<sup>8(a)</sup> and others.<sup>8(b)</sup> Defining a set of unique two-electron integrals is greatly facilitated by the results of the preceding section. Since in (13) and (14)

the two-electron integrals are multiplied by factors depending only on  $\vec{R}_\nu - \vec{R}_\mu$ , a minimum set will consist only of those integrals ( $ab|cd$ ) that possess unique spatial orientations of  $ab$  and  $cd$ , without regard to the absolute position of ( $ab|cd$ ). Thus, an integral involving four centers may be used four times (excluding consideration of point-group symmetry) by translating the indices of the integral such that the centers other than 1 may be taken to coincide with the origin.

This is seen more clearly by noting that a given integral

$$(\varphi^a(\vec{r})\varphi^b(\vec{r} - \vec{R}_\sigma) | \varphi^c(\vec{r} - \vec{R}_\mu)\varphi^d(\vec{r} - \vec{R}_\nu))$$

may be expressed equivalently as

$$(\varphi^a(\vec{r})\varphi^b(\vec{r} - \vec{R}_\sigma) | \{\vec{E} | -\vec{R}_\mu\} [\varphi^c(\vec{r})\varphi^d(\vec{r} - \vec{R}_\omega)]), \quad (16)$$

where  $\vec{R}_\omega = \vec{R}_\nu - \vec{R}_\mu$ . With cubic symmetry, there will be  $\sim \frac{1}{2}N^2/48$  distinct combinations of  $\vec{R}_\sigma$  and  $\vec{R}_\omega$ . This defines all unique angular orientations of  $\vec{R}_\omega$  with respect to  $\vec{R}_\sigma$ . The translation  $\{\vec{E} | \vec{R}_\mu\}$  provides radial separation of  $\vec{R}_\omega$  and  $\vec{R}_\sigma$ . Since each four-center integral may be used four times due to translational symmetry, there will be  $\sim N/4$  unique operations  $\{\vec{E} | \vec{R}_\mu\}$  for each choice of  $\vec{R}_\sigma$  and  $\vec{R}_\omega$ . As a result, the number of matrix elements requiring explicit evaluation is reduced from  $\sim \frac{1}{2}m^4N^3$ , as suggested by Eqs. (13) and (14), to only  $\sim \frac{1}{382}m^4N^3$ , a savings of over two orders of magnitude.

### III. EVALUATION OF ENERGY EXPRESSIONS

#### A. Repeating unit

Equations (13) and (14) represent general expressions for total energies and eigenvalues, but involve semi-infinite sums over atoms. Practical considerations dictate truncation of these sums and care is required to achieve a balance between one- and two-electron quantities such that rapid convergence may be attained. This situation is very similar to that in the classical Madelung problem, suggesting that rearrangement of the terms in the sums might be beneficial.

We begin by combining nuclear and electronic terms in Eq. (13) to obtain

$$E = N \sum_{\sigma} \left[ \frac{Z_{\sigma} Z_1 (1 - \delta_{1\sigma})}{2 |\vec{R}_{\sigma}|} + \sum_{a,b} D_{1\sigma}^{ab} \left( f h_{1\sigma}^{ab} + \sum_{\mu,\nu} \sum_{c,d} D_{\mu\nu}^{cd} [A(a^1 b^{\sigma} | c^{\mu} d^{\nu}) - B(a^1 c^{\mu} | b^{\sigma} d^{\nu})] \right) \right].$$

Noting that

$$\sum_{\sigma} \sum_{\mu}' \left\langle \varphi^a(\vec{r} - \vec{R}_{\sigma}) \left| \frac{Z}{|\vec{r} - \vec{R}_{\mu}|} \right| \varphi^b(\vec{r}) \right\rangle = \sum_{\omega} \sum_{\mu}' \left\langle \varphi^a(\vec{r} - \vec{R}_{\omega}) \left| \frac{Z}{|\vec{r}|} \right| \varphi^b(\vec{r} + \vec{R}_{\mu}) \right\rangle,$$

where the prime indicates  $\mu \neq 1$  in the sum and  $\vec{R}_{\omega} = \vec{R}_{\sigma} - \vec{R}_{\mu}$ , the sum may be partitioned as follows:

$$E/N = \sum_{a,b} \sum_{\sigma} D_{1\sigma}^{ab} \left( f \left\langle a^1 \left| -\frac{1}{2} \nabla^2 - \frac{Z}{|\vec{r}|} \right| b^{\sigma} \right\rangle + \sum_{c,d} \sum_{\nu} D_{1\nu}^{cd} [A(a^1 b^{\sigma} | c^1 d^{\nu}) - \frac{1}{2} B(a^1 c^1 | b^{\sigma} d^{\nu}) - \frac{1}{2} B(a^1 d^{\nu} | b^{\sigma} c^1)] \right) \quad (17a)$$

$$+ \sum_{a,b} \sum_{\sigma} \left( \frac{f}{2} D_{1\sigma}^{ab} \left\langle a^1 \left| \sum_{\mu}' \frac{-Z}{|\vec{r} - \vec{R}_{\mu}|} \right| b^{\sigma} \right\rangle + \frac{Z^2 (1 - \delta_{\sigma 1})}{|\vec{R}_{\sigma}|} \right) \quad (17b)$$

$$+ \sum_{c,d} \sum_{\mu} \sum_{\nu} D_{\mu\nu}^{cd} \left( \frac{f}{2} \left\langle c^{\mu} \left| \frac{-Z}{|\vec{r}|} \right| d^{\nu} \right\rangle + \sum_{\sigma} \sum_{a,b} D_{1\sigma}^{ab} [A(a^1 b^{\sigma} | c^{\mu} d^{\nu}) - \frac{1}{2} B(a^1 c^{\mu} | b^{\sigma} d^{\nu}) - \frac{1}{2} B(a^1 d^{\nu} | b^{\sigma} c^{\mu})] \right). \quad (17c)$$

The reasons for this choice of partitioning become apparent upon consideration of the properties of the  $D_{\mu\nu}^{ab}$  defined in Sec. II B. From the definition of  $\rho_{\nu}(\vec{r})$  we see that (17a) includes all Coulomb and exchange quantities resulting from the interaction of the local density at the origin with itself. In addition, there are terms describing the interaction of this local density with the nuclear charge at the origin. Thus, (17a) represents the self-energy of a neutral charge unit consisting of the local electron density and the associated

nucleus. Expression (17b) is the total energy of interaction between this unit and all other nuclei of the lattice, while (17c) represents the interaction between this unit and all other local electron densities. Collectively then, Eqs. (17) express the total energy as a sum of pairwise interactions between such neutral charge units centered at each site in the lattice.

In Fig. 1, we have plotted the density function  $\rho_1(\vec{r})$  along symmetry directions for a face-centered-cubic lattice of H atoms [lattice constant

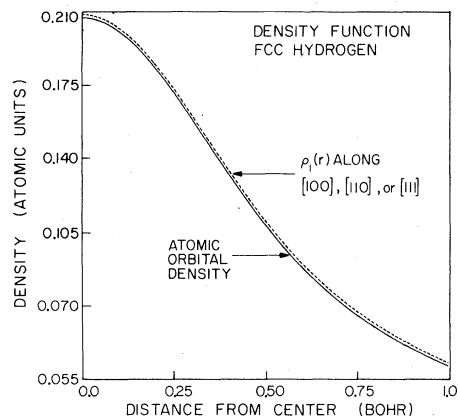


FIG. 1. Orbital density function  $\phi(\vec{r})\phi(\vec{r})$  and local density function  $\rho_1(\vec{r})$  for a face-centered-cubic lattice of hydrogen atoms. In this calculation,  $a=2.44 \text{ \AA}$  and  $\phi(\vec{r})$  is a  $1s$  basis function (with a nearest-neighbor overlap of 0.30). The calculation included 381 charge units. The relative shift of the two curves is real;  $\rho_1(\vec{r})$  becomes slightly negative at large distances, ensuring normalization.

$a=2.44 \text{ \AA}$  and  $\phi(r)$  is a  $1s$  basis function]. The  $D_{1\sigma}^{aa}$  values are highly peaked about the nucleus, producing a density function  $\rho_1(r)$  that extends with only small amplitude beyond the boundary of the Wigner-Seitz cell.

The partitioning of energy quantities in this fashion, while not unique, does clearly indicate the difficulties that might arise with straightforward truncation of (13). In using such a spherical cluster approach, two-electron integrals that retain all four indices within a radius  $R_\lambda$  of the origin are summed into the total energy. All nuclei within this radius are used in the computation of electron-nuclear (EN) attraction and nuclear-nuclear (NN) repulsion terms. As  $R_\lambda \rightarrow \infty$ , the correct limit is reached, but, in general, the convergence is very slow.<sup>9</sup> The reasons for this can be seen in Fig. 2(a). Here we show a particular atom  $\mu$  within a radius  $R_\lambda$  of the origin. A radius  $r'$  about  $\mu$  is indicated for which  $\rho_\mu(r)$  should be significant. For this atom, the EN and NN interactions with the charge unit at 1 will be fully counted, but only a portion of the interaction between  $\rho_\mu(r)$  and this unit will be included. Coulomb (and corresponding exchange) integrals of the form  $(a^\sigma b^1 | c^\mu d^\nu)$  for  $|\vec{R}_\nu| > R_\lambda$  are arbitrarily excluded, and thus the shaded portion of  $\rho_\mu(\vec{r})$  shown in the figure is omitted from the sum. Consequently, truncating the sum in this manner would be expected to produce an imbalance between one- and two-electron quantities. Indeed, Euwema *et al.*<sup>10</sup> employed such a method in a study of the diamond lattice and found it necessary to include monopole and dipole corrections to the potential in order to

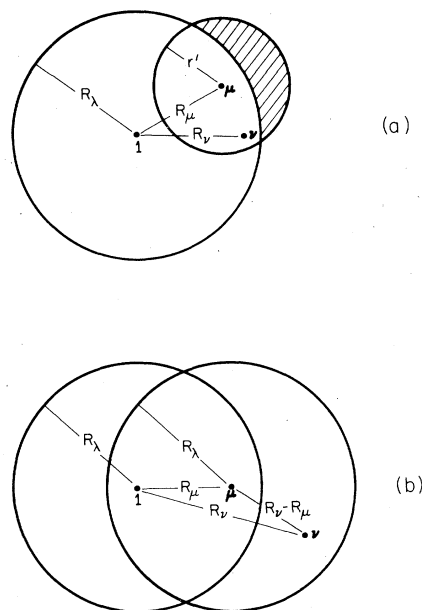


FIG. 2. (a) Schematic illustration of the spherical cluster approach. Integrals  $(a^\sigma b^1 | c^\mu d^\nu)$  are excluded when  $\nu$  is in shaded region. (b) In the bispherical cluster approach, electrons one and two are treated equivalently by including all centers  $\sigma$  and  $\nu$  such that  $|\vec{R}_\sigma| < R_\lambda$  and  $|\vec{R}_\nu - \vec{R}_\mu| < R_\lambda$ .

obtain adequate results.

The analysis leading to Eq. (17) suggests an alternate bispherical approach. Here, a sphere of radius  $R_\lambda$  is defined about each center  $\mu$  that is within  $R_\lambda$  of the origin. As before, all EN and NN interactions between the atoms  $\mu$  and the charge unit at the origin are included; however, to define repulsions between the  $\rho_\mu(\vec{r})$  and  $\rho_1(\vec{r})$ , all two-electron integrals  $(a^\sigma b^1 | c^\mu d^\nu)$  satisfying

$$|\vec{R}_\sigma| < R_\lambda, \quad |\vec{R}_\mu| < R_\lambda, \quad \text{and} \quad |\vec{R}_\mu - \vec{R}_\nu| < R_\lambda$$

are included. This arrangement of "bispherical" clusters is shown for a particular atom  $\mu$  in Fig. 2(b). Not only does this approach avoid charge imbalance, but it is also apparent that the sum need not be taken beyond the point where

$$\rho_1(\vec{R}_\mu/2) = \rho_\mu(\vec{R}_\mu/2) \ll 1,$$

since the charge unit at the origin is effectively shielded from all charge units farther away from the origin than  $|\vec{R}_\mu|$ .<sup>11</sup>

#### B. Balancing calculated quantities

Truncating the energy sums in any manner necessitates some modification of the concepts discussed in Sec. II. Partitioning the sums in the manner described above makes further discussion of the two-electron integrals particularly appro-

priate.

The discussion of charge units unambiguously defines the necessary two-electron contributions to Coulomb sums, but it is less clear concerning the unbiased evaluation of the exchange sums. The Hartree-Fock Hamiltonian provides a simple criterion for balancing Coulomb and exchange contributions since we must guarantee that

$$J_{\mathbf{k}_n, \mathbf{k}_n} - K_{\mathbf{k}_n, \mathbf{k}_n} = 0. \quad (18)$$

This cancellation of self-Coulomb and exchange terms is assumed to occur in deriving Eq. (8). Deviations from this condition are inherent in methods utilizing exchange approximations, and

the resultant residual Coulomb repulsions can seriously affect orbital shapes and total energies.<sup>12</sup> To examine this cancellation for *ab initio* methods, we first expand the expression (19) (leaving implicit the sums over  $a, b, c,$  and  $d$ ),

$$\begin{aligned} 0 &= J_{\mathbf{k}_n, \mathbf{k}_n} - K_{\mathbf{k}_n, \mathbf{k}_n} \\ &= \sum_{\sigma}^{N'} e^{i\mathbf{k} \cdot \mathbf{R}_{\sigma}} \sum_{\mu, \nu}^{N'} e^{i\mathbf{k} \cdot (\mathbf{R}_{\nu} - \mathbf{R}_{\mu})} \mathfrak{C} [(a^1 b^{\sigma} | c^{\mu} d^{\nu}) \\ &\quad - (a^1 c^{\mu} | b^{\sigma} d^{\nu})], \end{aligned}$$

where  $\mathfrak{C} = C^{*a} C^b C^{*c} C^d$ . This may be broken into six terms:

$$\sum_{\nu}^{N'} \mathfrak{C} e^{i\mathbf{k} \cdot \mathbf{R}_{\nu}} [(a^1 b^1 | c^1 d^{\nu}) - (a^1 c^1 | b^1 d^{\nu})], \quad \sigma=1, \mu=1 \quad (19a)$$

$$\sum_{\mu}^{N'} \mathfrak{C} e^{-i\mathbf{k} \cdot \mathbf{R}_{\mu}} [(a^1 b^1 | c^{\mu} d^1) - (a^1 c^{\mu} | b^1 d^1)], \quad \sigma=1, \mu \neq 1, \nu=1 \quad (19b)$$

$$\sum_{\mu, \nu}^{N'} \mathfrak{C} e^{i\mathbf{k} \cdot (\mathbf{R}_{\nu} - \mathbf{R}_{\mu})} [(a^1 b^1 | c^{\mu} d^{\nu}) - (a^1 c^{\mu} | b^1 d^{\nu})], \quad \sigma=1, \mu \neq 1, \nu \neq 1 \quad (19c)$$

$$\sum_{\sigma}^{N'} e^{i\mathbf{k} \cdot \mathbf{R}_{\sigma}} \sum_{\nu}^{N'} e^{i\mathbf{k} \cdot \mathbf{R}_{\nu}} \mathfrak{C} [(a^1 b^{\sigma} | c^1 d^{\nu}) - (a^1 c^1 | b^{\sigma} d^{\nu})], \quad \sigma \neq 1, \mu=1 \quad (19d)$$

$$\sum_{\sigma}^{N'} e^{i\mathbf{k} \cdot \mathbf{R}_{\sigma}} \sum_{\mu}^{N'} e^{-i\mathbf{k} \cdot \mathbf{R}_{\mu}} \mathfrak{C} [(a^1 b^{\sigma} | c^{\mu} d^1) - (a^1 c^{\mu} | b^{\sigma} d^1)], \quad \sigma \neq 1, \mu \neq 1, \nu=1 \quad (19e)$$

$$\sum_{\sigma}^{N'} e^{i\mathbf{k} \cdot \mathbf{R}_{\sigma}} \sum_{\mu, \nu}^{N'} e^{i\mathbf{k} \cdot (\mathbf{R}_{\nu} - \mathbf{R}_{\mu})} \mathfrak{C} [(a^1 b^{\sigma} | c^{\mu} d^{\nu}) - (a^1 c^{\mu} | b^{\sigma} d^{\nu})], \quad \sigma \neq 1, \mu \neq 1, \nu \neq 1. \quad (19f)$$

The sum restrictions over atoms used in each expression are shown at right. Of the six, (19a), (19b), and (19e) always cancel on a term-by-term basis. The same is true of (19f) if each integral included in the Coulomb (first) sum is also included in the appropriate position in the exchange (second) sum of that expression. Similarly, under these conditions, the Coulomb and exchange sums in (19c) will cancel exchange and Coulomb sums, respectively, of (19d) on a term-by-term basis. Thus, Eq. (18) will be satisfied exactly if each integral generated for summation into the Coulomb field of Eq. (13) is also entered into the correct position in the exchange sums. This is precisely the condition suggested by the partitioning of terms shown in Eq. (17).

#### IV. FACE-CENTERED-CUBIC HYDROGEN

In this section we present an application of the concepts discussed in the previous sections to a face-centered-cubic lattice of hydrogen atoms. Calculations were carried out using an expansion

of 1s Gaussians

$$\phi^a(r, \zeta) = \sum_{i=1}^P C_i e^{-\alpha_i r^2} / \sqrt{N_s}$$

on each center, where the coefficients  $C_i$  and  $\alpha_i$  are determined by fitting to a Slater orbital  $e^{-\zeta r}$  of scale parameter  $\zeta$ , and the number of functions ( $P$ ) in the expansion was allowed to be 1, 2, and 3. Both lattice constant  $a$  and scaling parameter  $\zeta$  were optimized, and we present a detailed discussion of the convergence and magnitude of the energy quantities involved in the  $\epsilon_{\mathbf{k}_n}$  and  $E/N$  sums.

##### A. Computational details

Both one- and two-electron matrix elements were generated using a program developed to incorporate all rotational and translational symmetries. The one-electron portion to Eq. (14) may be simplified to<sup>8(a)</sup>

$$\epsilon_{\mathbf{k}_n}^{\text{one}} = N \eta_{\mathbf{k}_n}^{-1} \sum_{a,b}^m \sum_{\lambda} h_{1\sigma(\lambda)}^{ab} C_{\mathbf{k}_n}^{*a} C_{\mathbf{k}_n}^b \sum_{\sigma}^{N_s} e^{i\mathbf{k} \cdot \mathbf{R}_{\sigma}}$$

where  $\sigma(\lambda)$  is an atom in shell  $\lambda$  and the inner sum is over the  $n_\lambda$  atoms in shell  $\lambda$ . For this case, only  $\lambda$  integrals  $h_{1\sigma}^{aa}(\lambda)$  are required. The symmetry properties of the density matrix allow processing of the two-electron integral list prior to

$$\begin{aligned}
 & N \sum_{a,b}^m \sum_{\sigma}^N D_{1\sigma}^{ab} \sum_{c,d}^m \sum_{\omega}^N D_{1\omega}^{cd} \sum_{\mu}^N [A(a^1 b^{\sigma} | \{\bar{\mathbf{E}} | -\bar{\mathbf{R}}_{\mu}\} \{c^1 d^{\omega}\}) - B(a^1 \{\bar{\mathbf{E}} | -\bar{\mathbf{R}}_{\mu}\} \{c^1\} | b^{\sigma} \{\bar{\mathbf{E}} | -\bar{\mathbf{R}}_{\mu}\} \{d^{\omega}\})] \\
 &= N \sum_{a,b}^m \sum_{\lambda} n_{\lambda} D_{1\sigma}^{ab} \sum_{c,d}^m \sum_{\lambda'} D_{1\omega}^{cd} \frac{1}{g_{\sigma}} \sum_j^{\mathcal{G}} \sum_{\mu}^N [A(a^1 b^{\sigma(\lambda)} | \{\bar{\mathbf{P}}_j | -\bar{\mathbf{R}}_{\mu}\} \{c^1 d^{\omega(\lambda')}\}) \\
 &\quad - B(a^1 \{\bar{\mathbf{P}}_j | -\bar{\mathbf{R}}_{\mu}\} \{c^1\} | b^{\sigma(\lambda)} \{\bar{\mathbf{P}}_j | -\bar{\mathbf{R}}_{\mu}\} \{d^{\omega(\lambda')}\})] \\
 &= N \sum_{a,b}^m \sum_{\lambda} n_{\lambda} D_{1\sigma}^{ab} \sum_{c,d}^m \sum_{\lambda'} D_{1\omega}^{cd} (A J_{1\sigma 1\omega}^{ab cd} - B K_{1\sigma 1\omega}^{ab cd}), \tag{20}
 \end{aligned}$$

where  $\bar{\mathbf{R}}_{\omega} = \bar{\mathbf{R}}_{\nu} - \bar{\mathbf{R}}_{\mu}$ . Here again  $\mathcal{G}$  is the lattice point group and  $g_{\sigma}$  is the appropriate degeneracy factor. The quantities  $J_{1\sigma 1\omega}^{ab cd}$  and  $K_{1\sigma 1\omega}^{ab cd}$  are independent of changes in the wave function, depending only on the choice of basis. For the largest case considered here ( $\lambda = 18$ ,  $N = 381$ ), truncating these sums in accordance with the definition of bispherical clusters produced an integrals list consisting of 324 values of  $J_{1\sigma 1\omega}^{aaaa}$  and 5184 values for the  $K_{1\sigma 1\omega}^{aaaa}$ .

A variety of sophisticated schemes have been developed for carrying out the sums over occupied states necessary to evaluate the density matrix elements.<sup>13</sup> Such schemes are necessary because evaluating the  $C_{\mathbf{k}n}^{\xi}$  values requires diagonalization of an  $m \times m$  matrix at each  $\mathbf{k}$  point to be considered. In these calculations  $m = 1$ , and no diagonalization is necessary. It is a relatively straightforward task in this case to carry out the sum by dividing the Brillouin zone into a fine grid of weighted volume elements, using an average value of  $\mathbf{k}$  for each element. The position of the Fermi surface was determined by noting the variation in  $\epsilon_{\mathbf{k}}$  in all directions radiating outward from the zone origin. The weights of elements intersected by the surface were made proportional to the volume enclosed. The actual summation (integration) was carried out using a simple Romberg procedure.<sup>14</sup> Some experimentation with grid size indicated that errors of  $O(10^{-4})$  hartree could be obtained with a grid of  $\sim 600$  points within  $\frac{1}{48}$ th of the total occupied portion of the zone.

In these calculations ( $m = 1$ ), the only task to be performed on an iterative basis is to achieve self-consistency in constructing the Fermi surface. Iterative changes in  $E/N$  and grid weights were monitored, and convergence to  $10^{-7}$  hartree and  $10^{-3}\%$ , respectively, could be obtained in a few

evaluation of the Hamiltonian matrix in a manner that greatly facilitates manipulation of these integrals. We will illustrate this by using (16) to rewrite (12) as

( $\leq 5$ ) iterations starting from a spherical Fermi surface.

## B. Results

To obtain a readily verifiable test of the stability and accuracy of the procedures used in this study, calculations were first carried out using a high-spin wave function (6) in the separated-atom limit ( $a = 40.0$  Bohr =  $21.16 \text{ \AA}$ ). Such a test is useful because in this limit  $\eta_{\mathbf{k}n} = N$  for all  $\mathbf{k}n$  and, since all states in the first Brillouin zone are filled,

$$D_{\mu\nu} = \sum_{\mathbf{k}n}^N \eta_{\mathbf{k}n}^{-1} e^{i\mathbf{k} \cdot (\bar{\mathbf{R}}_{\nu} - \bar{\mathbf{R}}_{\mu})} = \delta_{\mu\nu}.$$

This condition provides an exacting test of the integration procedure over the zone. In addition, we would expect to obtain

$$\epsilon_{\mathbf{k}n} = E/N = E_{\text{atom}}$$

for a high-spin wave function in the Ewald limit, where  $E_{\text{atom}}$  is the energy of an isolated hydrogen atom. This test was carried out using the two-function Gaussian 1s basis of Huzinaga<sup>15</sup> contracted for  $\zeta = 1.0$  (the free atom value). Eight shells of repeating units were considered ( $N = 135$ ), resulting in only eight unique nonzero two-electron integrals.<sup>16</sup> A grid of 1140 points was used in the Brillouin-zone integration. The calculated density matrix elements, listed in Table I, are within  $10^{-4}$  of the theoretical values. These errors propagate as shown in Table II, producing a total energy per atom and band spectrum deviating by no more than 0.00005 hartree from the theoretical value of  $-0.48581$ .

The optimum lattice parameter for the closed-shell (singlet) wave function was obtained from a series of HF calculations at different lattice

TABLE I. Density matrix values for a high-spin wave function in the separated-atom limit.<sup>a</sup> ( $N=135$ .)

	$\lambda$ (shell number)							
	1	2	3	4	5	6	7	8
$D_{1\sigma(\lambda)}^{aa}$	1.000 00	$1 \times 10^{-5}$	$2 \times 10^{-5}$	$2 \times 10^{-5}$	$1 \times 10^{-5}$	$-2 \times 10^{-5}$	$-1 \times 10^{-4}$	$4 \times 10^{-5}$

<sup>a</sup> Using the two-Gaussian basis from Ref. 15 with  $\xi=1.0$  and  $a=40.0$  bohrs.

spacings. As discussed below, 14 shells of charge units ( $N=249$ ) were adequate for this purpose, leading to  $E/N$  values within  $<0.001$  hartree of the largest systems considered. The two-function Huzinaga basis<sup>15</sup> was used on each atom, and the scaling parameter  $\xi$  was optimized for each value of  $a$  considered. The results of these calculations in terms of  $E/N$  and the virial ratio are shown for nine combinations of  $a$  and  $\xi$  in Table III. The optimum energy per atom of  $-0.4638$  hartree is unbound with respect to isolated H atoms ( $E = -0.4858$  hartree) by about 0.6 eV. This result is consistent (by the virial theorem) with an optimum exponent that is more diffuse ( $\xi=0.96$ ) than for an isolated H atom.

The behavior of energy quantities as a function of increasing  $N$  was examined in some detail. In Table IV are shown a variety of quantities obtained using optimum  $a$  and  $\xi$  for values of  $N$  between 13 and 381. In the first column,  $E/N$  values are given where in each case the Fermi surface was assumed to be completely spherical. The convergence, while not completely monotonic, is very rapid with the last three "clusters" differing in energy by less than 0.0004 hartree. Self-consistent energy values obtained after converging the Fermi surface are shown in the second column. It was expected initially that the iterative process might magnify errors inherent in the larger clusters; however, comparison of the two columns shows that this was not the case. Thus, it appears unlikely that addition of further shells would produce a change in this value by as much as 0.001 hartree.

More detailed information about convergence may be obtained by examining the individual terms in the energy sums. The terms listed in Tables V and VI are defined by recasting (14) in the simplified form

$$\begin{aligned} \epsilon_{\vec{k}_n} &= N\eta_{\vec{k}_n}^{-1} \sum_{\lambda} H_{1\sigma(\lambda)}^{aa} \sum_{\sigma}^{n_{\lambda}} e^{i\vec{k}\cdot\vec{R}_{\sigma}} \\ &= N\eta_{\vec{k}_n}^{-1} \sum_{\lambda} \left( h_{1\sigma(\lambda)}^{aa} + \frac{2}{f} (AJ_{1\sigma(\lambda)}^{aa} - BK_{1\sigma(\lambda)}^{aa}) \right) \sum_{\sigma}^{n_{\lambda}} e^{i\vec{k}\cdot\vec{R}_{\sigma}}, \end{aligned}$$

in which the innermost sum is over the  $n_{\lambda}$  atoms in a particular shell  $\lambda$ , and  $J_{1\sigma}^{aa}$  and  $K_{1\sigma}^{aa}$  include interactions with all other local density functions included in the calculation. A similar expression is possible for the total energy  $E$  in (13). The total Hamiltonian elements appear in Table V for selected values of  $\lambda$  from 2 to 18 ( $N=13$  to 381). A comparison of the matrix elements common to the  $N=225$  and  $N=381$  cases reveals that for all 13 matrix elements the discrepancies are no greater than 0.0005 hartree. Much of the difference between  $N=225$  and  $N=381$  total energies must be attributed simply to the additional terms in the  $N=381$  expansion.

The individual Coulomb and exchange matrix elements are grouped in Table VI. The Coulomb matrix elements for a given "cluster" tend towards zero with increasing  $\sigma(\lambda)$  at a rate proportional to the overlap terms  $S_{1\sigma(\lambda)}$ . The degree to which a given element deviates from zero in the converged limit is a measure of the non-point-charge character of the local density functions. It is an indication of the penetration of the charge units surrounding the origin into the unit at that point. The fact that these matrix elements approach a limiting value is an indication that this unit is fully shielded from all further additions.

The exchange matrix elements are larger in magnitude and tend towards zero more slowly than the corresponding Coulomb elements. An examination of Eqs. (13) and (14) shows that there are integrals of the form  $(1^a 1^a | \sigma^a \sigma^a)$  that contribute to

TABLE II. Total energy and band spectrum for a high-spin wave function in the separated-atom limit. ( $a=40a_0$  and  $N=135$ .)

Total energies		Eigenvalues at symmetry points				
$E/N$	$E_{\text{atom}}^a$	$\Gamma$	$X$	$W$	$L$	$K$
-0.485 81	-0.485 81	-0.485 84	-0.485 78	-0.485 81	-0.485 82	-0.485 81

<sup>a</sup> Using the two-Gaussian basis from Ref. 15 with  $\xi=1.0$ .

TABLE III. Optimization of lattice constant and scale factor for face-centered-cubic hydrogen.<sup>a</sup>

Lattice constant (Å)	Scale factor $\zeta$	Total energies $E/N$ (hartree)	$\epsilon_0$	$\epsilon_f^b$	Virial ratio
2.2376	0.90	-0.459 73	-0.9418	0.062	1.056 0
2.2376	1.00	-0.461 00	-1.0031	0.015	1.081 8
2.2376	1.10	-0.457 03	-1.0224	0.018	1.127 4
2.4614	0.90	-0.463 40	-0.9101	-0.061	0.975 64
2.4614	1.00	-0.463 07	-0.9325	-0.064	1.011 7
2.4614	1.10	-0.456 42	-0.9284	-0.032	1.071 8
2.6851	0.90	-0.460 55	-0.8721	-0.14	0.925 31
2.6851	1.00	-0.458 60	-0.8725	-0.12	0.973 02
2.6851	1.10	-0.449 25	-0.8560	-0.068	1.049 7
Optimum calculated values					
2.4388	0.958	-0.463 84	-0.9338	-0.0633	0.999 99

<sup>a</sup> Using a two-Gaussian expansion with  $N=249$ .

<sup>b</sup> The  $\epsilon_f$  values for all but the calculation at the optimum parameters are approximate and were obtained using a linear interpolation across the Fermi surface.

the matrix element  $K_{1\sigma(\lambda)}$  whose values dissipate as  $|\bar{R}_v|^{-1}$ . These are not, however, the predominant contributions to  $K_{1\sigma(\lambda)}$ , and the elements for large  $\sigma(\lambda)$  are negligibly small.

Finally, in Fig. 3 we show the calculated band spectrum and  $E/N$  for a calculation with  $N=381$  at the optimum lattice spacing. The  $P=3$  basis<sup>15</sup> was used with  $\zeta=0.958$  (the optimum value from the  $P=2$  basis). Comparison with the separated atom energy of  $-0.4970$  hartree indicates that at this level of calculation, the system is unbound by  $0.9$  eV.

#### V. SODIUM AND LITHIUM CONDUCTION BANDS

The application of real space basis-set expansion techniques has been limited for the most part to

ionic<sup>17</sup> or insulating systems<sup>10</sup> possessing very localized orbitals. The highly diffuse basis sets necessary to describe nearly-free-electron metal systems would be expected to produce poor convergence in conventional spherical cluster expansions. The definition of local electron density functions in the bispherical cluster approach provides a means by which this limitation might be eliminated. Accordingly, we have carried out additional calculations for the conduction band states of face-centered-cubic (fcc) sodium and lithium crystals, using the atomic orbital basis. This basis is too restricted to provide quantitative information about these conduction bands, but should illustrate the convergence properties of this technique.

TABLE IV. Total energies and band spectra for face-centered-cubic hydrogen as a function of cluster size.<sup>a</sup>

Shell number $\lambda$	No. of charge units $\sigma(\lambda)$	Total energy (hartree) <sup>b</sup>		Eigenvalues (hartree)		Virial ratio
		Spherical surface	Converged surface	$\epsilon_0$	$\epsilon_f$	
2	13	-0.537 9	-0.526 7	-0.737 9	-0.516 2	0.839 00
4	43	-0.456 1	-0.461 3	-0.876 1	-0.014 6	1.008 31
6	79	-0.457 2	-0.459 6	-0.911 0	-0.067 5	1.009 26
8	135	-0.462 09	-0.463 47	-0.927 74	-0.068 95	1.000 50
11	177	-0.462 31	-0.463 94	-0.933 28	-0.065 47	0.999 84
12	201	-0.462 21	-0.463 81	-0.934 44	-0.063 48	1.000 01
14	249	-0.462 26	-0.463 84	-0.933 84	-0.063 30	0.999 99
16	321	-0.462 57	-0.464 21	-0.930 22	-0.063 56	0.999 61
18	381	-0.462 62	-0.464 27	-0.927 57	-0.061 83	0.999 58

<sup>a</sup> Using a two-Gaussian expansion with  $\zeta=0.958$  and lattice constant  $a=2.44$  Å.

<sup>b</sup> Isolated atom energy is  $-0.4858$  hartree.

TABLE V. Total Hamiltonian matrix elements  $H_{1\sigma(\lambda)}$  for face-centered-cubic hydrogen.<sup>a</sup>

Shell no. $\sigma$	Magnitude	Charge units in calculation				
		43	135	225	321	381
1	$10^{-1}$	-4.6071	-4.6173	-4.6190	-4.6191	-4.6192
2	$10^{-1}$	-2.5683	-2.5806	-2.5811	-2.5812	-2.5812
3	$10^{-1}$	-1.1138	-1.1262	-1.1217	-1.1217	-1.1212
4	$10^{-2}$	-4.6785	-4.8401	-4.8480	-4.8476	-4.8490
5	$10^{-2}$	0.0	-2.0438	-2.0560	-2.0564	-2.0582
6	$10^{-3}$	0.0	-7.9322	-7.8527	-7.8572	-7.8461
7	$10^{-3}$	0.0	-3.3410	-3.3597	-3.3612	-3.3458
8	$10^{-3}$	0.0	-2.0588	-2.0359	-2.0303	-2.0319
9	$10^{-3}$	0.0	0.0	-1.5705	-1.5381	-1.5370
10	$10^{-4}$	0.0	0.0	-8.3562	-8.3783	-8.1912
11	$10^{-4}$	0.0	0.0	-8.9267	-8.9491	-9.0147
12	$10^{-4}$	0.0	0.0	-3.4751	-3.7483	-3.7957
13	$10^{-5}$	0.0	0.0	-2.1242	-3.6317	-2.9707
14	$10^{-4}$	0.0	0.0	0.0	1.4807	1.3651
15	$10^{-4}$	0.0	0.0	0.0	3.3233	3.2874
16	$10^{-4}$	0.0	0.0	0.0	3.1503	3.1738
17	$10^{-4}$	0.0	0.0	0.0	0.0	3.1900
18	$10^{-4}$	0.0	0.0	0.0	0.0	1.6276

<sup>a</sup> Using a two-Gaussian expansion with  $\zeta=0.958$  and lattice constant  $a=2.44 \text{ \AA}$ .

In these calculations, the core electrons were removed from the problem through the application of standard *ab initio* effective potential techniques.<sup>18</sup> Here, the one-particle equation for the valence orbital of the atom is written as

$$(-\frac{1}{2}\nabla^2 - Z/|r| + V^{\text{core}})\phi_v = \epsilon_v\phi_v,$$

where

$$V^{\text{core}} = \sum_{l,m=0}^{\infty} V_l(r) |l_m\rangle \langle l_m|$$

and each  $V_l(r)$  is a *local* potential describing the Coulomb and exchange interactions between the valence orbital  $\phi_v$  and the core orbitals. The functions  $V_l(r)$  are obtained from *ab initio* calculations on the atom, and the resultant orbital  $\phi_v$  cor-

TABLE VI. Hamiltonian components for face-centered-cubic hydrogen.<sup>a</sup>

Shell no. $\sigma$	Magnitude	Total Coulomb $h_{1\sigma(\lambda)}^{aa} + (2/f)J_{1\sigma(\lambda)}^{aa}$ Charge units					Total exchange $K_{1\sigma(\lambda)}^{aa}$ Charge units					
		43	135	225	321	381	Magnitude	43	135	225	321	381
1	$10^{-2}$	7.0405	5.9309	5.9104	5.9105	5.9062	$10^{-1}$	5.3111	5.2104	5.2100	5.2101	5.2098
2	$10^{-2}$	-5.6655	-5.9749	-5.9808	-5.9808	-5.9821	$10^{-1}$	2.0018	1.9831	1.9831	1.9831	1.9830
3	$10^{-2}$	-3.6024	-3.7045	-3.7065	-3.7065	-3.7070	$10^{-2}$	7.5352	7.5576	7.5103	7.5108	7.5046
4	$10^{-2}$	-1.9367	-1.9756	-1.9762	-1.9762	-1.9764	$10^{-2}$	2.7418	2.8644	2.8717	2.8714	2.8726
5	$10^{-3}$	0.0	-9.7403	-9.7418	-9.7417	-9.7423	$10^{-2}$	0.0	1.0697	1.9818	1.0822	1.0840
6	$10^{-3}$	0.0	-4.3849	-4.3849	-4.3849	-4.3851	$10^{-2}$	0.0	3.5474	3.4678	3.4723	3.4611
7	$10^{-3}$	0.0	-1.9421	-1.9421	-1.9421	-1.9422	$10^{-2}$	0.0	1.3989	1.4176	1.4191	1.4037
8	$10^{-4}$	0.0	-8.5856	-8.5849	-8.5844	-8.5847	$10^{-3}$	0.0	1.2002	1.1774	1.1718	1.1735
9	$10^{-4}$	0.0	0.0	-3.7313	-3.7310	-3.7309	$10^{-3}$	0.0	0.0	1.1974	1.1650	1.1640
10	$10^{-4}$	0.0	0.0	-1.5580	-1.5577	-1.5577	$10^{-4}$	0.0	0.0	6.7982	6.8206	6.6336
11	$10^{-4}$	0.0	0.0	-1.5580	-1.5577	-1.5577	$10^{-4}$	0.0	0.0	7.3687	7.3914	7.4570
12	$10^{-5}$	0.0	0.0	-6.4636	-6.4618	-6.4615	$10^{-4}$	0.0	0.0	2.8287	3.1021	3.1495
13	$10^{-5}$	0.0	0.0	-2.6881	-2.6873	-2.6873	$10^{-6}$	0.0	0.0	-5.6389	9.4435	2.8339
14	$10^{-5}$	0.0	0.0	0.0	-1.1114	-1.1115	$10^{-4}$	0.0	0.0	0.0	-1.5919	-1.4762
15	$10^{-6}$	0.0	0.0	0.0	-4.5120	-4.5206	$10^{-4}$	0.0	0.0	0.0	-3.3685	-3.3326
16	$10^{-6}$	0.0	0.0	0.0	-4.5122	-4.5208	$10^{-4}$	0.0	0.0	0.0	-3.1954	-3.2190
17	$10^{-7}$	0.0	0.0	0.0	0.0	-7.6948	$10^{-4}$	0.0	0.0	0.0	0.0	-3.1977
18	$10^{-7}$	0.0	0.0	0.0	0.0	-3.0129	$10^{-4}$	0.0	0.0	0.0	0.0	-1.6306

<sup>a</sup> Using a two-Gaussian expansion with  $\zeta=0.958$  and lattice constant  $a=2.44 \text{ \AA}$ .

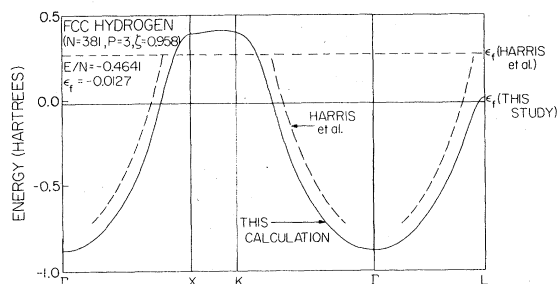


FIG. 3. Band spectrum along symmetry directions for face-centered-cubic hydrogen using  $N=381$  and a three-Gaussian expansion (Ref. 15) for the  $1s$  orbital.

rectly mimics the character of a valence orbital obtained with all core electrons explicitly included in the calculation.

#### A. Computational details

Under standard conditions, both sodium and lithium exist in body-centered cubic lattices.<sup>19</sup> Both metals undergo a martensitic transition at low temperature, which for lithium produces a partial conversion to a fcc structure. The fcc structure is thought to be favorable for sodium at low temperature,<sup>20</sup> although it has not been observed.

The fcc lithium structure has been characterized with  $a=4.370$  Å, representing a 1.88% expansion of the nearest neighbor distance relative to the bcc phase.<sup>19</sup> This distance was used in calculations on the fcc lithium structure, while for sodium, bond distances for the bcc lattice were scaled outward by 1.88% to obtain  $a=5.343$  Å. The effective potentials and basis sets used were those of Melius and Goddard.<sup>18</sup> For both sodium and lithium, the valence orbital consisted of four Gaussian expansions in which the three most contracted functions used coefficients found optimum for the atom. The coefficient for the most diffuse Gaussian was optimized in the band calculations involving 135 charge units.<sup>18</sup> The optimum

basis sets were then used in calculations of up to 249 charge units to assess the convergence of energetic quantities. In addition, the lattice parameter  $a$  was optimized for each metal in calculations with  $N=135$ .

#### B. Results and discussion

Energy quantities for the four largest clusters considered ( $N=177$  to 249) are collected in Tables VII and VIII for sodium and lithium, respectively. Comparison with trends in Table IV suggests that  $E/N$  values are converged to within 0.001 hartree, while Fermi energies and bandwidths are only slightly less reliable. Overlap values  $S_{1\mu}^{aa}$  are collected in Table IX, together with those of the two-Gaussian hydrogen basis, and indicate the insensitivity of the bispherical method to the diffuse character of the metal basis sets.

The reasons for this insensitivity may be seen by examining Fig. 4. Here we show the  $\rho_v(\vec{r})$  function for lithium along several symmetry directions, together with the corresponding atomic orbital density function  $\phi(\vec{r})\phi(\vec{r})$ . While the overlap values of Table IX suggest that the  $\rho_v(\vec{r})$  function might extend to very long range, the figure indicates that it is very similar in shape to the atomic orbital density. It is the oscillating nature of the  $D_{1\nu}^{aa}$  values that results in the highly localized nature of  $\rho_v(\vec{r})$ .

As indicated by Fig. 5 and Table X, the calculated band spectra for these systems deviate only slightly from a totally spherical distribution, in agreement with experimental information.<sup>21</sup> Work function values for lithium and sodium may be estimated from Fermi energies  $\epsilon_f$ , listed in Tables VII and VIII (using  $\lambda=14$ ), and correcting for the potential shift due to the metal surface.<sup>22</sup> Values calculated in this manner (0.2 and 1.2 eV) are smaller than the observed values for bcc lithium and sodium (2.49 eV [Ref. 23(a)] and 2.26 eV [Ref. 23(b)]). To some extent, the error is a result of simple basis-set deficiencies, particularly

TABLE VII. Total energies and band spectra for face-centered-cubic lithium as a function of cluster size.<sup>a</sup>

Shell number $\lambda$	No. of charge units $\sigma(\lambda)$	Total energy (hartree) <sup>b</sup>		Eigenvalues (hartree)	
		Spherical surface	Converged surface	$\epsilon_0$	$\epsilon_f$
11	177	-0.178 49	-0.179 95	-0.305 52	0.035 34
12	201	-0.178 17	-0.179 55	-0.303 24	0.046 25
13	225	-0.177 91	-0.179 29	-0.301 12	0.051 75
14	249	-0.177 71	-0.179 13	-0.299 52	0.054 49

<sup>a</sup> Using the atomic orbital from Ref. 18 and a lattice constant of  $a=4.370$  Å.

<sup>b</sup> Isolated atom energy with effective potential is -0.1964 hartree.

TABLE VIII. Total energies and band spectra for face-centered-cubic sodium as a function of cluster size.<sup>a</sup>

Shell number $\lambda$	No. of charge units $\sigma(\lambda)$	Total energy (hartree) <sup>b</sup>		Eigenvalues (hartree)	
		Spherical surface	Converged surface	$\epsilon_0$	$\epsilon_f$
11	177	-0.165 97	-0.166 88	-0.280 01	-0.014 40
12	201	-0.165 89	-0.166 75	-0.280 12	-0.011 99
13	225	-0.165 85	-0.166 72	-0.279 87	-0.011 23
14	249	-0.165 85	-0.166 71	-0.279 57	-0.010 97

<sup>a</sup> Using the atomic orbital from Ref. 18 and a lattice constant of  $a = 5.343 \text{ \AA}$ .

<sup>b</sup> Isolated atom energy with effective potential is  $-0.1819$  hartree.

in the region near the Fermi surface.

The result of lattice optimizations are shown in Table XI where the optimum lattice constant for lithium is found to be  $5.17 \text{ \AA}$ , 17% larger than the experimental value, and the system is unbound by  $0.2 \text{ eV}$  per atom. The calculated bulk modulus of  $8.37 \times 10^{10} \text{ dynes/cm}^2$  is comparable to the experimental bcc value<sup>24</sup> ( $11.6 \times 10^{10} \text{ dynes/cm}^2$ ) and is quite weak, indicating that large changes in bond distances will be accompanied by relatively small energy changes. Thus we might expect significant improvements in the calculated value of  $a$  with modest improvement of wave-function quality. Similar considerations apply to the sodium lattice. Here, the calculated lattice constant is expanded by 11% relative to the estimated fcc value, and the lattice is unstable by  $0.3 \text{ eV}$ .

## VI. DISCUSSION

### A. Comparison with other methods

The high symmetry and infinite periodicity of a three-dimensional lattice allow the crystalline HF problem to be considered from within a variety of different representations. Of those investigators who have formulated the problem in real space, Calais and Sperber<sup>25</sup> have described a method that bears the closest resemblance to our own. They

arrived at the same choice of repeating density unit through consideration of the properties of the density matrix<sup>25 (c)</sup>; however, their evaluation of the total energy was quite different. Whereas we have chosen to integrate the field experienced by a single unit cell over all space, Calais and Sperber integrate the field due to all atoms in the lattice over a single Wigner-Seitz cell. While elegant, the resulting integrations are difficult and make self-consistent evaluation of coefficients and the Fermi surface less practical.

Euwema *et al.*<sup>10</sup> have carried out calculations on the diamond lattice using the spherical cluster method. Some consideration is given in that paper to the definition of a minimum set of two-electron integrals within the constraints of the method. As mentioned earlier, they approach the problem of charge imbalance inherent in the spherical cluster method through the application of monopole and dipole corrections to the potential. The calculations so defined are carried out self-consistently, producing optimum orbital coefficients and zone point weights for the integration in  $k$  space.

Several methods utilize a Fourier representation. Mauger and Lannoo<sup>26</sup> utilize the Fourier transform of an LCAO (Bloch) wave function. Brener and Fry<sup>27</sup> expand the Coulomb potential in a Fourier series and the exchange operator as

TABLE IX. Overlap values using optimum basis sets.

Shell number	2	4	6	8	10	12
Shell coordinates (in lattice units)	(110)	(211)	(310)	(321)	(330)	(420)
Sodium <sup>a</sup>	0.359 68	0.060 08	0.013 21	0.003 32	0.000 90	0.000 48
Lithium <sup>b</sup>	0.444 54	0.104 53	0.029 45	0.009 15	0.003 01	0.001 76
Hydrogen <sup>c</sup>	0.298 43	0.037 03	0.005 04	0.000 70	0.000 10	0.000 04

<sup>a</sup> Lattice constant =  $5.343 \text{ \AA}$ .

<sup>b</sup> Lattice constant =  $4.370 \text{ \AA}$ .

<sup>c</sup> Lattice constant =  $2.439 \text{ \AA}$ . (Two-Gaussian expansion with  $\zeta = 0.958$ .)

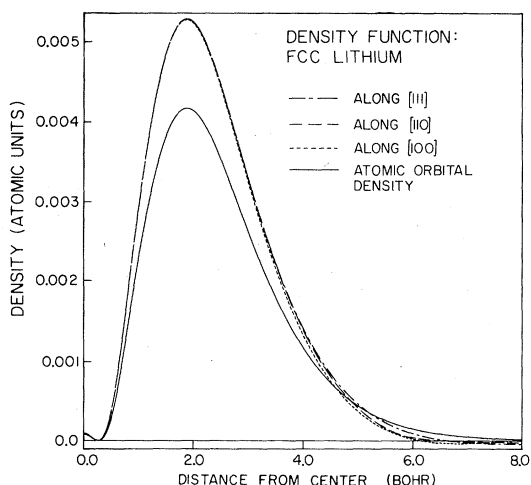


FIG. 4. Orbital density function and local density function for a face-centered-cubic array of lithium atoms. The experimental lattice parameter of  $a = 4.370 \text{ \AA}$  was used in a calculation with  $N = 249$ .

a double Fourier integral. To overcome slowly converging sums, the overlapping atomic potential approximation is invoked to obtain the core contributions to the sums.

The method of Harris *et al.*<sup>28</sup> is most directly comparable to the one described here, as it is formulated with the intention of providing results in the Ewald limit, and has been applied to both the hydrogen and lithium problems discussed here. They have chosen a formalism in which the Coulomb potential is expressed as a Fourier transform, producing energetic quantities in terms of weighted lattice sums of orbital products. The method involves considerable numerical complexity and is limited to systems involving a single occupied band.<sup>29(a)</sup> As current Fourier representation methods do not permit the use of *ab initio* effective potential techniques, a zero-differential

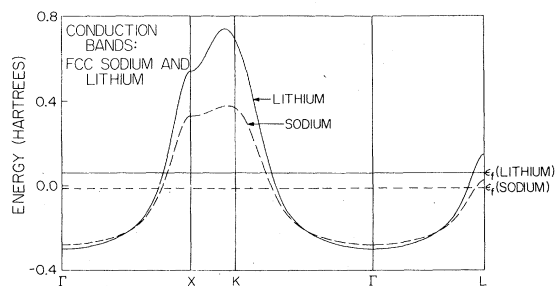


FIG. 5. Conduction-band spectra for sodium and lithium along symmetry directions. Both calculations involved 249 charge units at the experimental face-centered-cubic lattice separation and both were carried out using the optimized basis sets.

TABLE X. Comparison of  $k_f$  values between calculated and spherical (free-electron) Fermi surfaces.

System	$k_f$ values at symmetry points		
	K	X	L
Hydrogen <sup>a</sup>	0.777 59	0.769 15	0.825 85
Lithium <sup>b</sup>	0.782 77	0.784 57	0.776 59
Sodium <sup>c</sup>	0.776 21	0.781 42	0.796 70
Free electron	0.781 59	0.781 59	0.781 59

<sup>a</sup> Using  $P = 3$  basis set and  $a = 2.44 \text{ \AA}$ .

<sup>b</sup> Using optimum four-Gaussian basis and  $a = 4.370 \text{ \AA}$ .

<sup>c</sup> Using optimum four-Gaussian basis and  $a = 5.343 \text{ \AA}$ .

overlap approximation is invoked in the treatment of core states.<sup>28,30(a)</sup>

Unlike the real-space techniques, the method of Harris *et al.* is able to economically utilize Slater-type orbitals, and this is done in the studies of hydrogen<sup>29</sup> and lithium.<sup>30</sup> In Fig. 3 we show the calculated band spectrum for hydrogen obtained by this method for comparison with our own. While the shapes are quite similar, there is clearly a discrepancy in the absolute position of the band spectrum. Although Harris *et al.* do not report energies near the  $\Gamma$  point, total energies are quoted and the system is found to be unbounded by a measure (0.9 eV) identical to that obtained here. Since total electronic energies of a restricted HF wave function may be expressed as

$$E = \sum_{\vec{k}_n}^{Np/f} f(\epsilon_{\vec{k}_n} + h_{\vec{k}_n, \vec{k}_n})/2,$$

the similarity in total energies and disparity in band spectra are surprising. Our calculated lattice constant of  $2.44 \text{ \AA}$  is somewhat longer than the  $2.24 \text{ \AA}$  obtained in the Harris *et al.* study, and the optimum scale parameters of 0.96 and  $\sim 1.25$ , respectively, are quite different. Based on the virial theorem, one would expect an unbound system to yield a  $\zeta$  smaller than the free atom, and it is difficult to understand why their value is larger. These differences could arise from the somewhat different form of Bloch wave functions employed by Harris *et al.*<sup>28</sup>

Because of the use of a single (contracted)  $s$  function on each atom, our lithium results are of limited quantitative value; however, some comparisons with the results of Kumar *et al.*<sup>30</sup> are valuable. In that study, numerical instabilities in the normal procedures required fitting results to a free-electron, logarithmic exchange term in order to obtain  $\epsilon_*$ . Thus, full band spectra were not reported; however, the limiting values  $\epsilon_f$  and  $\epsilon_0$  were quoted. Their band spectrum is shifted upwards by about 0.1 hartree relative to our comparable results at the optimum lattice spacing shown in Table XI. The calculated bandwidth in

TABLE XI. Lattice-constant optimization for sodium and lithium. ( $N = 135$ .)

Metal	Lattice constant (Å)	Energy (hartree)	Eigenvalues (hartree)		Bulk modulus ( $10^{10}$ dynes/cm <sup>2</sup> )
			$\epsilon_0$	$\epsilon_f$	
Sodium	5.244	-0.163 77	-0.296 6	-0.007 3	7.67
	5.774	-0.169 05	-0.302 5	-0.038 3	
	6.303	-0.167 76	-0.287 5	-0.049 7	
		Optimum values			
	5.934	-0.171 36	-0.285 32	-0.045 5	
Lithium	4.688	-0.185 39	-0.319 3	-0.002 2	8.37
	5.005	-0.187 68	-0.326 1	-0.024 5	
	5.323	-0.187 72	-0.328 9	-0.045 3	
		Optimum values			
	5.169	-0.188 11	-0.332 0	-0.039 4	

that study of 0.265 hartree is also somewhat different from our own (0.293 hartree). While these differences may be due to choice of basis set, it is relevant to note that the optimum lattice parameter obtained in that study is 5.45 Å, considerably larger than that obtained here. A similar discrepancy is observed in comparing the bcc results of Calais and Sperber<sup>25(a)</sup> ( $a = 7.0$  a.u.) with those of Kumar *et al.*<sup>30</sup> ( $a = 8.2$  a.u.). This comparison is particularly relevant in that both methods employ Slater-type atomic orbitals, differing only in the treatment of core orbitals and the form of Bloch expansion used. While Kumar *et al.*<sup>30</sup> attribute the discrepancy to the differences in Bloch expansions, the extremely small change in energy obtained with variation of  $a$  raises some concern about the validity of the core approximation used by Kumar *et al.*<sup>30</sup>

#### B. On generalization to lesser periodicity

As mentioned at the outset, the development of this HF procedure was conceived as a first step in producing more general methods capable of dealing with lesser periodicity. Emphasis has been placed on numerical simplicity and stability and maximizing the use of existing, mathematically straightforward techniques of theoretical chemistry. There are a variety of ways in which this formalism might be generalized to two-dimensional systems:

(1) Two-dimensional Bloch basis functions of the form

$$\varphi_{\vec{k}_\parallel}^a(l, \vec{r}) = \sum_{\mu} e^{i\vec{k}_\parallel \cdot \vec{R}_\mu} \phi^a(\vec{r} - \vec{R}_\mu - \vec{R}_l)$$

may be used, where  $\vec{R}_l$  determines the origin of a particular layer in the slab,  $\vec{R}_\mu$  is measured from

that origin within the layer, and  $\vec{k}_\parallel$  is a two-dimensional wave vector. One-electron wave functions are

$$\psi_{\vec{k}_\parallel, a_{n\perp}}(\vec{r}) = \eta_{\vec{k}_\parallel, a_{n\perp}}^{-1/2} \sum_a C_{\vec{k}_\parallel}^a \sum_l C_{a_{n\perp}}^a(l) \varphi_{\vec{k}_\parallel}^a(l, \vec{r}),$$

where a separate coefficient  $C_{a_{n\perp}}^a$  is needed to define oscillations in the direction perpendicular to the surface (there will be  $l$  values of  $q$  for each bound  $n$ ). Within the formalism defined here, such functions would lead to the definition of a two-dimensional local density function and manipulation would be much the same as discussed above. For slabs of a sufficient number of layers, the local density functions at one face could be constrained to be those of a bulk calculation, thereby eliminating the artificial "thickness" phenomena characteristic of a slab calculation.

(2) For systems in which localized bonding or pair correlation effects are important, it would be more effective to define a basis for a compound unit cell extending through the thickness of the slab,

$$\varphi_{q_\perp}^a(\omega, \vec{r}) = \sum_{\mu} C_{q_\perp}^a \phi^a(\vec{r} - \vec{R}_\omega - \vec{R}_\mu),$$

where  $\vec{R}_\omega$  locates the compound cell origin and the  $\vec{R}_\mu$  locate atoms within the cell from that origin. There will be as many values of  $q_\perp$  as there are atoms in the cell possessing a particular  $\phi^a(\vec{r})$ . The coefficients  $C_{q_\perp}^a$  are fixed and are chosen so as to make the  $\varphi_{q_\perp}^a(\omega, \vec{r})$  orthogonal for a given choice of  $a$  and  $\omega$ . One-electron functions become

$$\psi_{\vec{k}_\parallel, a_{n\perp}}(\vec{r}) = \eta_{\vec{k}_\parallel, a_{n\perp}}^{-1/2} \sum_{\omega} e^{i\vec{k}_\parallel \cdot \vec{R}_\omega} \times \left( \sum_a C_{\vec{k}_\parallel}^a \sum_{q_\perp} C_{a_{n\perp}}^a \varphi_{q_\perp}^a(\omega, \vec{r}) \right).$$

In this way, all the information relevant to a single compound cell may be isolated by the terms in brackets. Linear combinations of such orbitals could be used effectively in describing correlation effects in a generalized valence bond wave function.<sup>7</sup>

(3) Noting that the matrix elements  $H_{10}^{aa}(\lambda)$ , discussed in Sec. IV B contain all of the Hamiltonian information relevant to a pair of atoms separated by  $|\vec{R}_1 - \vec{R}_v(\lambda)|$ , one may design a finite-cluster method in which the atoms are "unaware" that they are set in a finite lattice. Using these elements to define a zero-order Hamiltonian matrix between atoms, the finite cluster would experience the field of an infinite surrounding array (when corrected for the neighboring atoms included explicitly). Thus interstitial migration or vacancy formation could be treated rigorously as a correction to this Hamiltonian.

Loss of periodicity in the direction perpendicular to the surface necessarily leads to the generation of more nonunique two-electron matrix elements in methods (1) and (2). From the results of both semiempirical<sup>1</sup> slab calculations and *ab initio* cluster calculations<sup>2(a)</sup> it appears unlikely that sufficient layers will be required for this to be of serious consequence.

#### ACKNOWLEDGMENTS

This research was carried out with partial support from the U. S. Department of Energy Grant No. EX-76-G-03-1305. However, any opinions, findings, conclusions, or recommendations expressed herein are those of the authors and do not necessarily reflect the views of the DOE. Partial support was obtained from a Grant (DMR 79-19689) from the National Science Foundation.

<sup>1</sup>See, for example: (a) F. J. Arlinghaus, J. G. Gay, and J. R. Smith, in *Theory of Chemisorption*, edited by J. R. Smith (Springer, New York, in press); (b) J. Ferrante and J. R. Smith, *Phys. Rev. B* **19**, 3911 (1979).

<sup>2</sup>(a) T. H. Upton, W. A. Goddard III, and C. F. Melius, *J. Vac. Sci. Technol.* **16**, 531 (1979); (b) G. T. Surratt and A. B. Kunz, *Phys. Rev. Lett.* **40**, 347 (1978).

<sup>3</sup>W. A. Goddard III, J. J. Barton, A. Redondo, and T. C. McGill, *J. Vac. Sci. Technol.* **15**, 1274 (1978).

<sup>4</sup>C. F. Melius, T. H. Upton, and W. A. Goddard III, *Solid State Commun.* **28**, 504 (1978).

<sup>5</sup>C. C. J. Roothaan and P. S. Bagus, *Methods Comput. Phys.* **2**, 47 (1963).

<sup>6</sup>For the wave functions indicated,  $\chi_{HS} = \alpha \alpha \alpha \alpha \dots \alpha$ ,  $\chi_{CS} = \alpha \beta \alpha \beta \alpha \beta \alpha \beta \dots$ .

<sup>7</sup>F. W. Bobrowicz and W. A. Goddard III, in *Modern Theoretical Chemistry: Methods of Electronic Structure Theory*, edited by H. F. Schaefer III (Plenum, New York, 1977), Vol. 3, pp. 79-127.

<sup>8</sup>(a) J. C. Slater and G. F. Koster, *Phys. Rev.* **94**, 1498 (1954); (b) M. Miasek, *Bull. Acad. Pol. Sci. CI*, III, **4**, 805 (1956).

<sup>9</sup>T. H. Upton and W. A. Goddard III (unpublished).

<sup>10</sup>R. N. Euwema, D. L. Wilhite, and G. T. Surratt, *Phys. Rev. B* **7**, 818 (1973).

<sup>11</sup>It is appropriate to consider the limiting behavior of the energy sums. This question has been considered in some detail for ionic lattices. It has been shown [F. E. Harris, *Ref. 28*; R. N. Euwema and G. T. Surratt, *J. Phys. Chem. Solids* **36**, 67 (1975); A. Redlack and J. Grindlay, *ibid.* **36**, 73 (1975)] that conditionally convergent sums approach the Ewald or infinite crystal limit if the repeating unit has net-zero dipole moment and second-moment trace. For nonionic systems with continuous charge distribution, as are treated here, a moment expansion [F. W. De Wette and B. R. A. Nijboer, *Physica* **24**, 1105 (1958)] reveals that the neutral charge unit need only have vanishing dipole and quad-

rupole moments to converge absolutely.

<sup>12</sup>S. J. Niemczyk and C. F. Melius, *Chem. Phys. Lett.* **46**, 236 (1977).

<sup>13</sup>(a) H. J. Monkhorst and J. D. Pack, *Phys. Rev. B* **13**, 5188 (1976); (b) D. J. Chadi and M. L. Cohen, *ibid.* **8**, 5747 (1973).

<sup>14</sup>See, for example, C. F. Gerald, *Applied Numerical Analysis* (Addison-Wesley, Reading, Mass. 1978), pp. 212-214.

<sup>15</sup>S. Huzinaga, *J. Chem. Phys.* **42**, 1293 (1965).

<sup>16</sup>For large interatomic separation, only those integrals ( $a^1 b^1 c^1 d^1$ ) that scale as  $|\vec{R}_\mu|^{-1}$  are nonzero. For eight shells of repeating units, there will be eight such unique integrals.

<sup>17</sup>A. B. Kunz and N. O. Lipari, *Phys. Rev. B* **4**, 1374 (1971).

<sup>18</sup>C. F. Melius and W. A. Goddard III, *Phys. Rev. A* **10**, 1528 (1974). The coefficients used with the most diffuse (fourth) Gaussians were  $C_4(\text{Na}) = 0.26480$  and  $C_4(\text{Li}) = 0.32840$ .

<sup>19</sup>W. P. Pearson, *A Handbook of Lattice Spacings and Structure of Metals and Alloys* (Pergamon, New York, 1958).

<sup>20</sup>C. S. Barrett, *Am. Mineral.* **33**, 749 (1948); *J. Inst. Met.* **84**, 43 (1955).

<sup>21</sup>D. L. Randles and M. Springford, *J. Phys. F* **3**, L185 (1973).

<sup>22</sup>N. D. Lang and W. Kohn, *Phys. Rev. B* **3**, 1215 (1971).

<sup>23</sup>(a) P. A. Anderson, *Phys. Rev.* **75**, 1205 (1949); (b) E. Patai, *Z. Phys.* **59**, 697 (1930).

<sup>24</sup>K. A. Gschneidner, Jr., *Solid State Phys.* **16**, 276 (1964).

<sup>25</sup>(a) J. L. Calais and G. Sperber, *Int. J. Quantum Chem.* **7**, 501 (1973); (b) G. Sperber and J. L. Calais, *ibid.* **7**, 521 (1973); (c) G. Sperber, *ibid.* **7**, 537 (1973).

<sup>26</sup>A. Mauger and M. Lannoo, *Phys. Rev. B* **15**, 2324 (1977).

<sup>27</sup>N. E. Brener and J. L. Fry, *Phys. Rev. B* **17**, 506

(1978).

<sup>28</sup>F. E. Harris, *Theor. Chem.: Adv. Perspect.* 1, 147 (1975). "Modulated plane-wave" Bloch functions of the form

$$\psi_{\vec{k}}^j(\vec{r}) = e^{2\pi i \vec{k} \cdot \vec{r}/a} \sum_{\vec{\mu}} \phi_j(\vec{r} - a\vec{\mu})$$

are used in this paper and in Refs. 29 and 30.

<sup>29</sup>(a) F. E. Harris, L. Kumar, and H. J. Monkhorst, *Phys. Rev. B* 7, 2850 (1973); (b) D. E. Ramaker, L. Kumar, and F. E. Harris, *Phys. Rev. Lett.* 34, 812 (1975).

<sup>30</sup>(a) L. Kumar, H. J. Monkhorst, and F. E. Harris, *Phys. Rev. B* 9, 4084 (1974); (b) L. Kumar and H. J. Monkhorst, *J. Phys. F* 4, 1135 (1974).